University of Nebraska - Lincoln

DigitalCommons@University of Nebraska - Lincoln

2022

Optimization and Standardization of DMS Chemical Mapping Experiments for Probing RNA 3D Structure

Sarah Brady
University of Nebraska - Lincoln

Optimization and standardization of DMS chemical mapping experiments for probing RNA 3D structure

An Undergraduate Honors Thesis
Submitted in Partial fulfillment of
University Honors Program Requirements
University of Nebraska-Lincoln

By
Sarah Brady, BS, BA
Microbiology
Music Performance
College of Arts and Sciences
College of Fine and Performing Arts

March 11, 2022

Faculty Mentors:
Joseph Yesselman, PhD, Chemistry
Brandi Sigmon, PhD, Microbiology

Table of Contents

Abstract

RNA plays a significant and crucial role in biological processes. The properties of RNA are ultimately responsible for each molecule's unique function. The configuration and structural integrity of RNA is important for its functionality. Chemical mapping detailed in this thesis can be used to analyze the 3D structure of an RNA sequence. RNA is modified via methylation of adenine and cytosine bases using dimethyl sulfate, then reverse transcribed to DNA, then sequenced. The sites where the bases were methylated become mutations in the DNA sequence, allowing for identification of these locations when analyzing sequencing data. Conditions for modification can be altered to provide insight into the structure of the compound in vitro. This thesis details optimizations and changes made to chemical mapping protocols to increase data accuracy, experiment reproducibility, and efficiency. The major changes made include altering of modification time and amount of dimethyl sulfate (DMS) used, increasing magnesium amounts added to the reaction to aid in folding, and altering of purification methods and DNA processing.

Key Words

RNA tertiary structure, chemical mapping optimization, RNA modification, RNA 3D structure, tertiary contacts, dimethyl sulfate (DMS), chemical mapping

Introduction

Importance of 3D RNA structure

Structured RNAs are important for biological function by the role they play in biosynthesis and metabolism (Sharp 2019). Contrary to DNA, RNA has the intriguing capability to act as an enzyme and play a role in other biological functions including transcription and translation of the genetic code (Sharp 2019). The key behind the functionality of structured RNA lies in its 3D structure. Base pairing interactions between nucleotides of an RNA molecule are responsible for secondary RNA structure that is characterized by repeating sequences, or motifs. These motifs can be loops, helices, or junctions and contribute to the functionality of 3D structured RNA (Leontis, Lescoute, Westhof 2006). Long range interactions between secondary structure motifs create tertiary contacts. Current experimental methods show great accuracy at predicting secondary RNA structure and identification of RNA motifs. However, the determination of 3D structure is more difficult because of tertiary contact formation. The formation of tertiary contacts is not well understood, making predictability of 3D structure more difficult. Improvements to predicting tertiary contact formation will allow a greater understanding of 3D RNA structure. Much of the enzymatic RNA's role within the cell, and as targets for cancer and disease, can be explained through its 3D structure (Kurrek 2009). This information could be applied to formulate a practical model of tertiary RNA structure, which would be a critical step forward in fully understanding the significance and role of RNA in biological systems.

Current experiments to determine RNA structure

Current experiments to probe RNA structure include nuclear magnetic resonance (NMR), cryo-EM, x-ray crystallography, and crosslinking. Cryo-EM and X-ray crystallography are high resolution methods, however both are time consuming to complete. RNA crosslinking and chemical mapping are lower resolution methods but are much faster than cryo-EM and crystallography (Demme et. al. 2022). Resolution of chemical mapping has been improved by coupling the experiment with next-generation sequencing. The data from chemical mapping gives resolution at the nucleotide level, allowing for observation of base pair interactions. This information can be applied to the analysis of tertiary structures in a way RNA crosslinking is not able to achieve.

The chemical mapping experiment

Chemical mapping probes RNA structure through chemical modifications to nucleotides that are dependent upon the structural environment. Chemical mapping has widely been used in secondary structure determination by probing base pairing interactions. This thesis outlines a novel use of chemical mapping procedures to probe tertiary RNA structure (Figure 2). Chemical mapping is useful in gathering information about 3D RNA conformation and folding because modification is dependent upon the position of nucleotides to be modified.

The standardized experiment involves RNA modification using dimethyl sulfate (DMS). DMS adds a methyl group to solvent accessible adenine bases at the N1 position and cytosine bases at the N3 position (Figure 1). Solvent accessible nucleotides for modification are strongly dependent upon the structure of the RNA. Base pairing interactions, including hydrogen bonding or tertiary contact involvement, decrease molecular solvent accessibility. Adenine and cytosine bases involved in these interactions are not expected to be methylated by DMS. There should be very few methylations to these bases from DMS if these bases are involved in other interactions because the N1 of adenine and the N3 of cytosine cannot be accessed by the DMS. DMS methylations to adenine and cytosine nucleotides that are unpaired and not involved in molecular interactions (e.g. base pairing, loops, or tertiary contacts) should be quite high, as these bases will be solvent accessible to DMS (Figure 1). The formation of tertiary contacts can be quantified with chemical mapping data to better understand the role they play in tertiary structure.
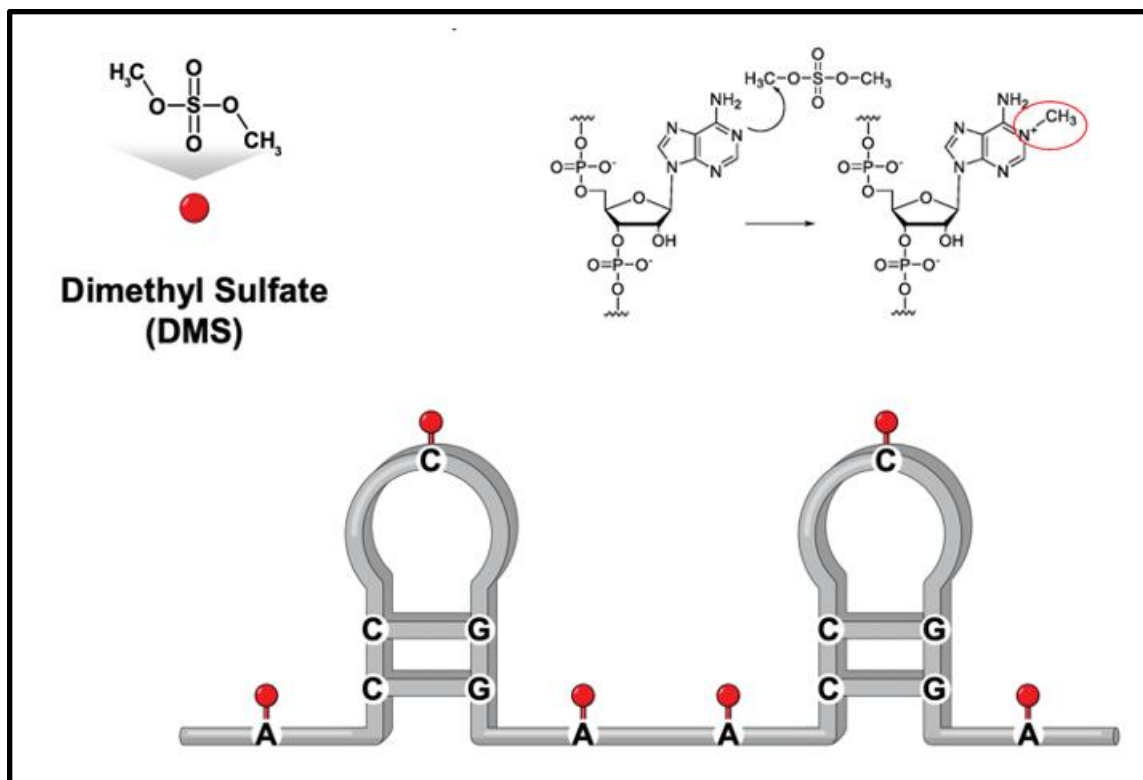
Figure 1. Dimethyl sulfate chemically modifies adenine bases at the N1 position, and cytosine bases at the N3 position to solvent accessible nucleotide bases. The red circles indicate DMS and show modification to adenine and cytosine bases on an RNA molecule.

Once RNA is modified and solvent accessible adenine and cytosines are methylated, the RNA is reverse transcribed. Reverse transcription is a process that generates complementary DNA from a single RNA strand. This process mirrors that of typical transcription within a living cell, but instead of an end product of RNA, the end product is complementary DNA (cDNA). When the modified RNA undergoes reverse transcription, the methylated nucleotides cannot be used by the reverse transcriptase to generate this cDNA. A nonsense base is put in place of the nucleotide in the complementary DNA strand when reverse transcription occurs. Barcodes are added to the construct by the reverse transcriptase at the end of the sequence to coordinate the sequencing data to the specific experiment. This cDNA can then be amplified using polymerase chain reaction (PCR). PCR creates double stranded DNA. Sequencing adapters can now be added to the sample and underdog Next-Generation sequencing. Sequencing the DNA allows for the order of nucleotides to be determined in each construct that is sequenced. The mutations in the DNA caused by the DMS modification sites are recognizable after sequencing, and data analysis allows

mutation rates of nucleotide bases to be compared to a non-modified sequence with no mutations to determine the overall reactivity of the bases.

Data analysis is largely dependent upon a barcode process used to sort sequenced samples. Each RNA has a common end sequence that primer DNA will complement. A short strand of ten nucleotides after this end sequence is the barcode. The barcode is on the reverse transcription primer, so when the construct is primed, the barcode is added. This is crucial to the data analysis process because each barcode is unique to an RNA and correlates to an individual experiment. Once data from the sequencer is obtained, Novocraft is used to demultiplex the information. Novocraft uses the barcodes on each sequence to sort each read into a folder that corresponds to its respective code (and therefore a unique sequence). When the information for each RNA is sorted to correspond to its specific experiment, data is aligned. Bowtie2 attempts to match the known, original target sequence to the data from the sequencer. Bowtie2 counts the number of mismatches per number of reads. This value is a fraction and shows what fraction of the nucleotides are modified at each base location. This fraction gives valuable information about the amount of modification at each site. If a base is very solvent accessible, one can expect a very high fraction of mismatches per number of reads. If a base is completely inaccessible to solvent, one can expect a very low fraction of mismatches per number of reads. Data for DMS analysis is compared to conditions with no DMS modification to compare the mismatch levels when DMS is used in comparison to water. There are very few mutations in the DNA without the DMS, showing DMS is responsible for the mutations seen in the sequencing data.

The strength of tertiary contacts can be determined from this chemical mapping data when certain conditions (e.g., reaction temperature, chemical modifier concentration, reaction time, etc.) are manipulated. This can provide indications for the overall structure of the molecule and what variables have the greatest impact on the RNA molecule's structure. Using chemical mapping as a way to elucidate tertiary structure brings many challenges that have now been circumvented, which are detailed in this thesis. These improvements are pertinent because they improve an extremely useful and powerful experiment. The changes made drastically cut down experiment length, allowing for greater ease of data collection and greater advancement into the study of RNA tertiary structure.
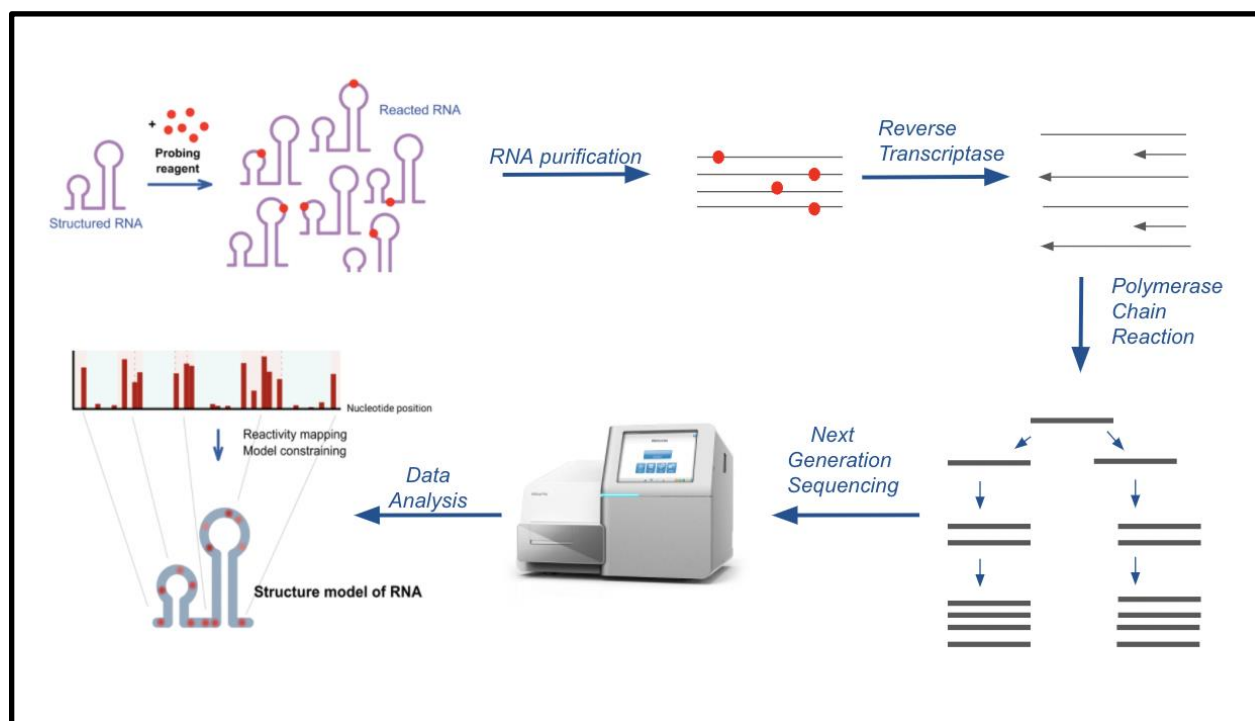
Figure 2. Graphic of the chemical mapping experiment.

Importance of chemical mapping optimization, applications to microbiology/bioinformatics fields
Optimization of this experiment streamlines experimental research, increases reproducibility of results, and ensures accurate findings for implications of RNA molecule structure. The findings of chemical mapping experiments allow for contribution to information about RNA tertiary structure, and ultimately provide specific implications for microbiological and medical disciplines. It allows us to better understand diseases and gene expression, providing insight into the effectiveness of various drugs. An example of a therapeutic application of structural RNA findings relates to small RNAs. Small RNAs (sRNAs) are small bacterial molecules that play a significant role in gene expression within microbes and membrane protein regulation. If the 3D structure of these sRNAs in bacterial cells can be elucidated, it would have large contributions to the development of antibacterials and treatment of bacterial disease. If the gene expression can be blocked, membrane protein regulation could be impaired, stopping cell growth and division and ultimately slowing or preventing disease development. Applications can also include performing DMS modification at a pH of 8, which deprotonates guanine and uracil bases, allowing DMS to modify all four

nucleotides. This type of chemical probing was first explored in *Escherichia coli,* delineating a route to in vivo studies (Mustoe et. al. 2019).

Methods

Changes made from original protocol

Changes to chemical mapping protocols in existing literature were made based on efficiency, cost, and accuracy and improvement of results of the experiment as a whole. The changes to the original experiment and the reasoning for doing so are as follows:

1. Amount of Magnesium added to RNA samples during folding stage of experiment. Originally, constructs were folded with a folding buffer and 8mM $MgCl_2$. The optimized experiment now uses 10mM $MgCl_2$, 20% more than original protocols, during the folding stage of the experiment. The folding buffer used is sodium cacodylate ($C_2H_7AsO_2$). The concentration of magnesium increased in the optimized experiment because metal ions greatly increase the stability of RNA folding. The positive ion charge counteracts the highly negative charges from the phosphates that can put pressure on the molecule when folded.

2. Amount of DMS and modification time. First protocols added 5uL of a 90uL EtOH, 9uL H_2O, and 1uL DMS mixture and modified at room temperature for 15 minutes before being quenched to stop the methylation modifications. The now standardized optimized protocol uses 2.5uL of a 85uL EtOH, 15uL DMS mixture and modifies the RNA sample for 6 minutes. Sequencing results using these modification conditions were more accurate with less background noise.

3. Altering Buffer Conditions. Existing literature shows the use of 0.35 M sodium cacodylate as a folding buffer for the chemical mapping experiment.The high sodium content of 0.25 M sodium cacodylate is not closely related to biological cell conditions and works exclusively in vitro. Hepes buffer (4-(2-hydroxyethyl)- 1-piperazineethanesulfonic acid) is closer to biological conditions in comparison to sodium cacodylate. Findings indicate the experiment works with a wide range of buffers, reflected in figure 5.

4. DNA processing via PCR and gel extraction. In order to ensure concentrations of DNA were high enough for product and sequencing, PCR was performed and gel extractions from a 2% agarose gel were used to capture the greatest amount of sample possible. Q5

Platinum Hot Start Polymerase was used for the PCR. Optimal conditions for this enzyme led to 16-18 cycles being the ideal amount for gel extraction of the sample. Using precast e-gels (with the capability to perform band excisions) is possible and the best option for most RNA constructs, and was used most often to streamline procedures and save time. However, if higher concentrations of product are needed for sequencing, a casted gel is used to ensure more samples are obtained. PCR purification is a viable alternative to gel extraction, however could result in more off product in the final DNA sample used for sequencing.

5. Methods of RNA and DNA purification. dT beads (Dynabeads) were the first method of purification. The use of dT beads resulted in significantly more loss of product due to unintentional pipetting error during sample purification. Purification practices shifted from the use of these beads in ethanol washes to a new method using nucleic acid spin purification kits. Literature suggests equivalency between spin purification kits and ethanol washes using dT beads.

Results

Optimized experiment

Below describes the optimized conditions and methods for the chemical mapping experiment for 3D structure determination. These were determined through the optimization experiments performed (see "Methods").

RNA Preparation & Folding.

1. Use diluted RNA between 4 uM and 8 uM to begin the experiment.
2. Add 5uL of diluted RNA to a PCR tube for the number of conditions being used. Run for 4 minutes at a 90C heat and immediately after run for 3 minutes at 4C.
   a. If using one construct but titrating multiple variables, put the RNA all in one tube for the Heat and Cool, then divide into 5uL respectively for each tube.
3. Create folding buffer mix following table below:

#	REAGENT	CONC	VOL (UL)	N VOL(UL)
1	Sodium Cacodylate	0.4 M	16.5	

2	MgCl2	250 mM	1.0	

4. Add 17.5 uL of folding buffer into each tube.

5. Let RNA fold for 30 minutes at room temperature.

RNA Modification and Purification.

6. Prepare DMS mix following table below:

#	REAGENT	CONC	VOL (UL)	N VOL(UL)
1	DMS	-	15	15.00
2	100% EtoH	-	85	85

7. Add 2.5 uL of DMS mix into each tube. Allow modification for 6 minutes.

8. Quench each tube with the addition of 25 uL of 2-mercaptoethanol (BME).

9. Purify samples using the RNA Clean and Concentrator -5 Kit from Zymo Research (catalog number R1013) according to the instructions in the kit. Elute in 7uL of H_2O.

10. Measure RNA concentration using ThermoFisher Qubit RNA Broad Range Assay according to the instructions in the kit.

Reverse Transcription.

11. Prepare reverse transcription mix following table below:

#	REAGENT	CONC	VOL (UL)	N VOL(UL)
1	TGIRT buffer	5x	2.4	
2	dNTPs	10 mM	1.2	
3	DTT	0.1 M	0.6	
4	TGIRT-III Enzyme	280 U/uL	0.5	

12. Pipette 4.7 uL of RT mix into new PCR tubes.

13. Add purified RNA according to its Qubit concentration. RNA amounts in uL = 1/RNA concentration in uM. This step may require addition of H_2O to reach the correct amount for reverse transcription at a total total volume of 6.4 uL in each reaction tube.

14. Add reverse transcription primers. Each condition should have its own unique barcode primer; keep track of which primer barcode corresponds to its respective construct. Add 1 uL of 0.285 uM primer to each tube.

15. Allow reverse transcription to run at 57C for 2 hours.

16. Add 5 uL of 0.4M NaOH to each tube.

17. Run for 4 minutes at a 90C heat and immediately after run for 3 minutes at 4C.

18. Add 2.5 uL of Quench Acid mix: 2mL of 5M NaCl, 2mL of 2M HCl, and 3mL of 3M Na-acetate. This can be prepared prior to the experiment and stored at room temperature.

19. Purify this complementary DNA using the Oligo Clean and Concentrator kit from Zymo Research according to the instructions in the kit. Elute in 15 uL of H_2O.

Downstream PCR.

20. Prepare PCR mix as follows in table below:

#	REAGENT	CONC	VOL (UL)	N VOL(UL)
1	2x q5 master mix	2X	25	
2	H2O	-	18	

21. Add 43 uL of q5 PCR mix into each tube.

22. Add 2 uL of purified DNA into respective tubes.

23. Add 2.5 uL of forward PCR primer and 2.5 uL reverse PCR primer for each tube.

24. Run the PCR according to the table.

	STAGE	TEMP	TIME	CYCLES
	Initial Denaturation	98 C	30 secs	1
	Denaturation	98 C	10 secs	
	Annealing	62 C	15 secs	
	Extension	72 C	15 secs	16
	Final Extension	72 C	5 mins	
	Hold	4 C	INF	

Gel purify DNA for sequencing

25. Run samples on an e-gel. Use Invitrogen e-gel EX 2% casted agarose gels. Use 20 uL of NEB low molecular weight ladder in one lane to ensure constructs are correct.

    a. For lanes with sample, add 15 uL of e-gel loading buffer and 5 uL of sample. These should be prepared on a 96-well plate and 20 uL in total added into the gel lanes.

    b. For any lanes without sample, add 20 uL of loading dye. The gel does not run properly without extra lanes filled with loading dye or H_2O.

       c.   Run 2% gel for 10 minutes. Export image with USB drive from imager.

26. Perform a band excision on the gel. Break open the plastic gel, cut out the bands of interest using the backlight on Invitrogen gel imager. Place excised bands in new tubes (one sample per tube).

27. Purify DNA with DNA Gel Recovery Kit from Zymo Research according to kit instructions.

28. Elute in 25 uL of 10mMTris-HCl (pH 8.5) then do a second spin with another 25 uL to ensure all the product is collected. Elution should be 50 uL in total.

29. Measure DNA concentration using ThermoFisher Qubit DNA 1x High Sensitivity assay according to the instructions in the kit.

30. Dilute each sample to 1 nM according to Qubit concentrations. 1 nM concentration is needed for Next-Generation Sequencing.

31. Measure DNA concentration using Qubit DNA 1x High Sensitivity assay according to kit instructions to record final concentration for sequencing.

Impacts of the changes made as detailed in the "Methods" section above.

1. <u>Amount of Magnesium added to RNA samples during the folding stage of experiment.</u>

Below are results comparing the same construct. Figure 3A shows a lower fraction of modification from DMS with 0.313 mM magnesium added during folding. Figure 3B shows higher levels of DMS modification with 5mM of magnesium in the folding buffer.
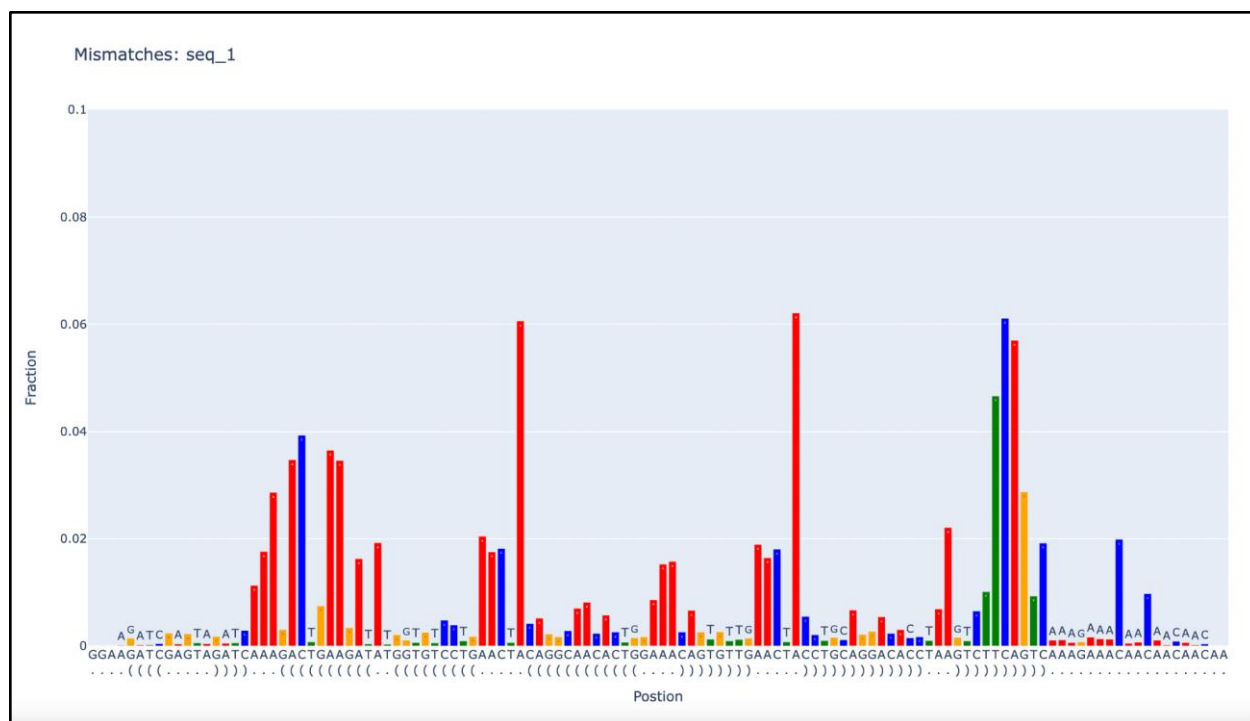
Figure 3A. Fraction of modifications for RNA construct with 0.313mM Mg2+ added during folding. Red represents adenine bases, blue represents cytosine bases. The horizontal axis shows which nucleotide corresponds to what reactivity, and the vertical axis shows what percentage of nucleotides at that position were methylated by DMS.
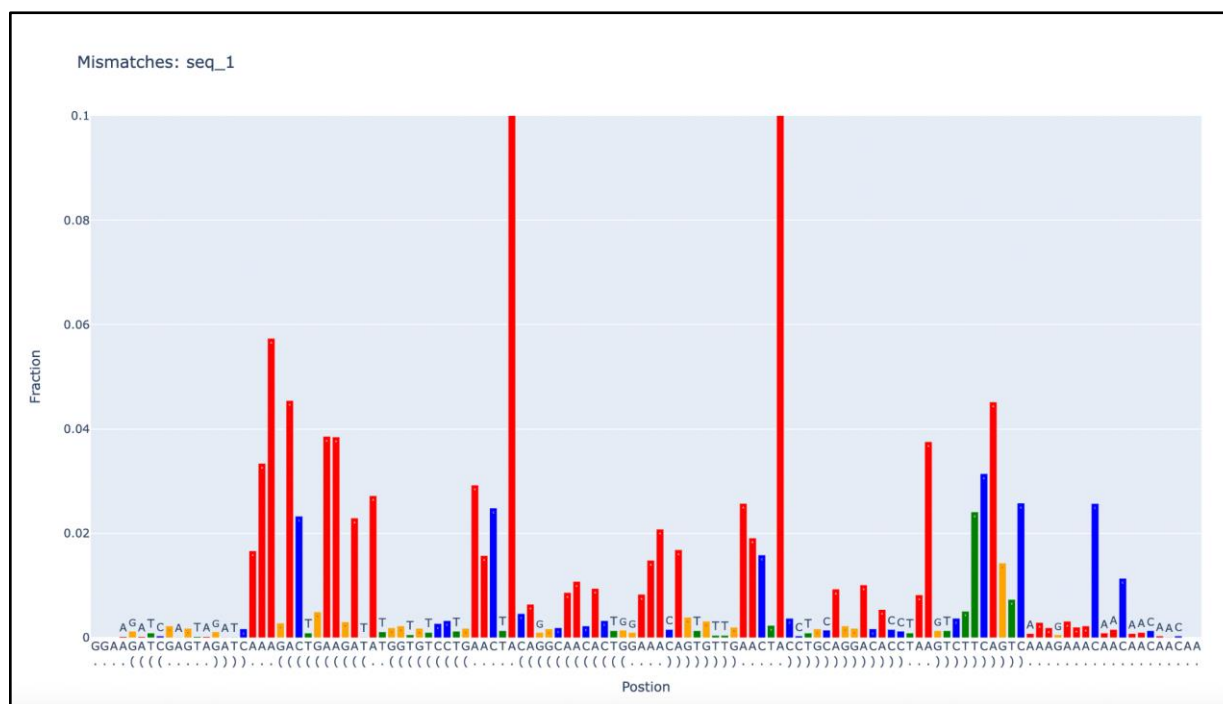
Figure 3B. Fraction of modifications for RNA construct with 5 mM Mg2+ added during folding. Red represents adenine bases, blue represents cytosine bases. The horizontal axis shows which nucleotide corresponds to what reactivity, and the vertical axis shows what percentage of nucleotides at that position were methylated by DMS.

2. Increase in DMS amount, decrease in modification time.

The figures below compare the same construct with titrated modification time and DMS concentration. As the amount of DMS used for modification decreased, modification time increased. Results show DMS mix 3 (96.25 uL of EtOH and 3.75 uL of DMS) with a modification time of 7 minutes had modification of a tertiary contact within the structure. DMS mix 1 (85 uL EtOH and 15 uL of DMS) with a modification time of 3 minutes also showed promising modification patterns. DMS mix 5 (90 uL H_2O, 9 uL EtOH, and 1 uL DMS) showed little modification of solvent accessible adenine and cytosine bases.
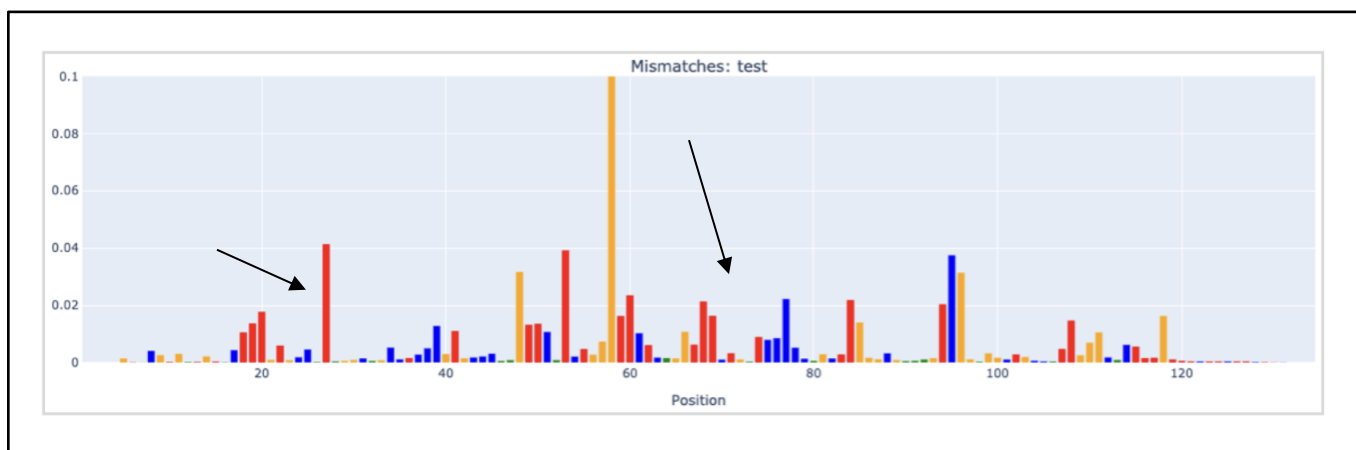
Figure 4A. DMS mix 1 modified for 3 minutes. Fractions of modification of tertiary contacts are noted.
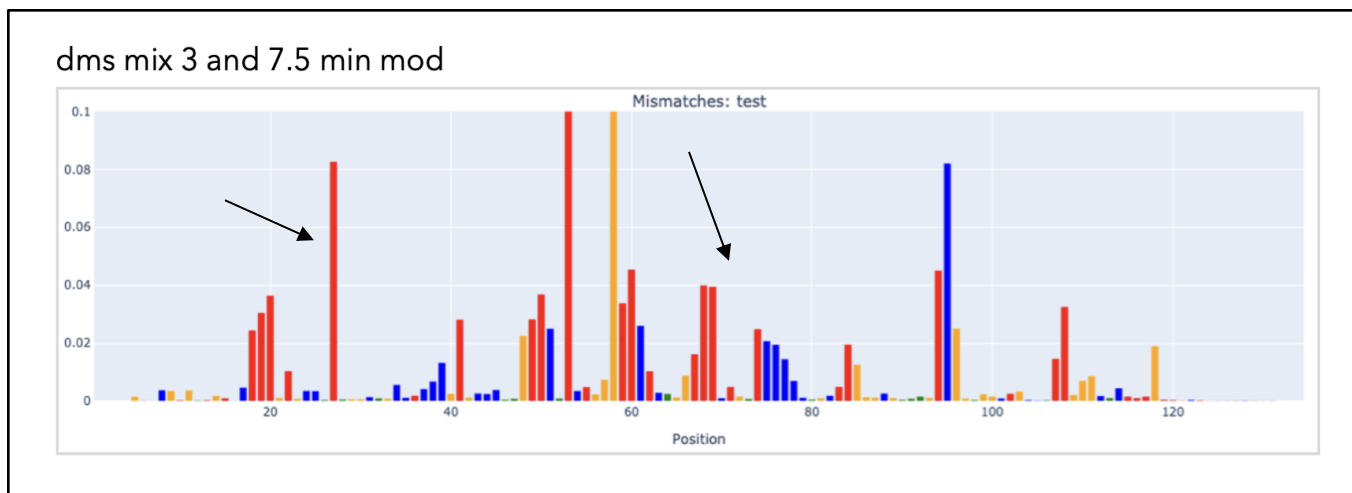
Figure 4B. DMS mix 3 modified for 7.5 minutes. Fractions of modification of tertiary contacts are noted.
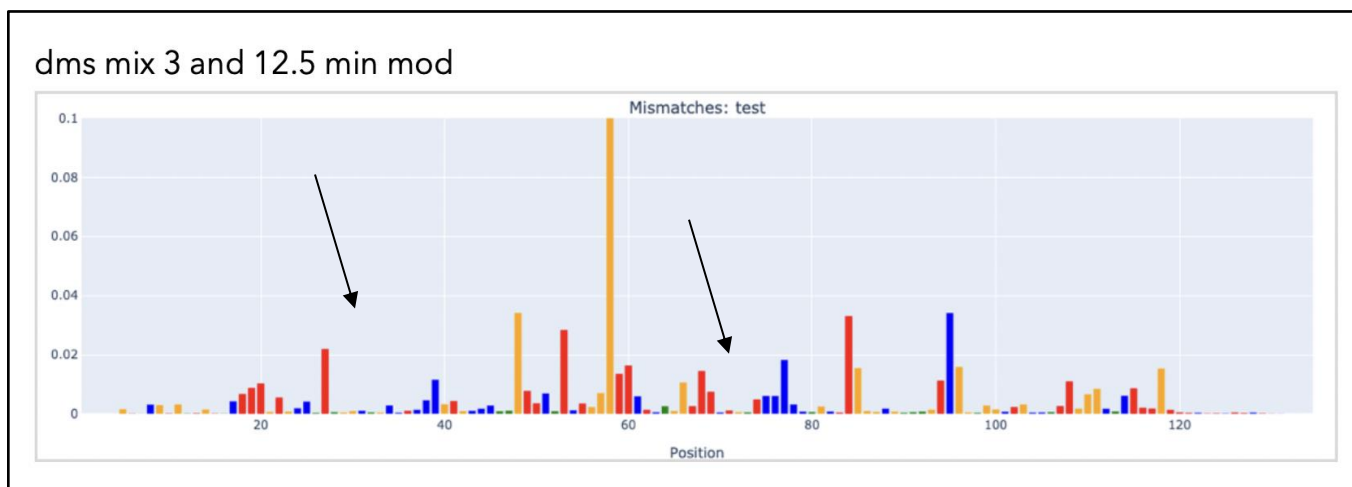

Figure 4C. DMS mix 3 modified for 12.5 minutes. Fractions of modification of tertiary contacts are noted.
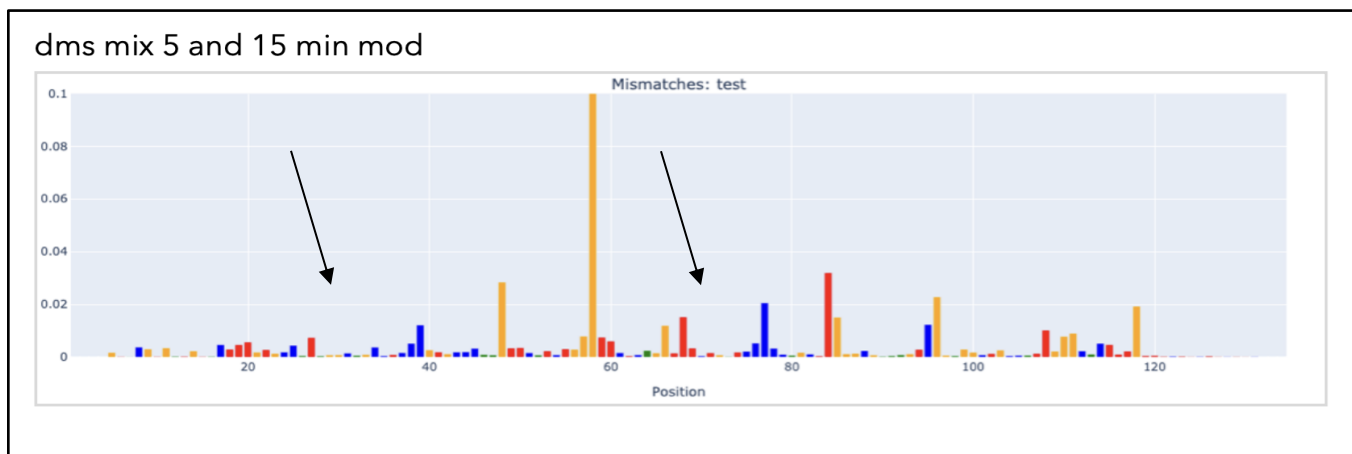
Figure 4D. DMS mix 5 modified for 15 minutes. Fractions of modification of tertiary contacts are noted.

3. Comparing folding buffers sodium cacodylate to HEPES

Figure 5A shows chemical mapping data using the previously used 0.35 M sodium cacodylate folding buffer. Although effective in modification, this high sodium content is not closely related to biological cell conditions and works only exclusively in vitro. Results show folding buffers creating conditions close to biological conditions are still capable of promoting successful chemical modification, as seen in Figure 5B using 0.05 M sodium cacodylate.
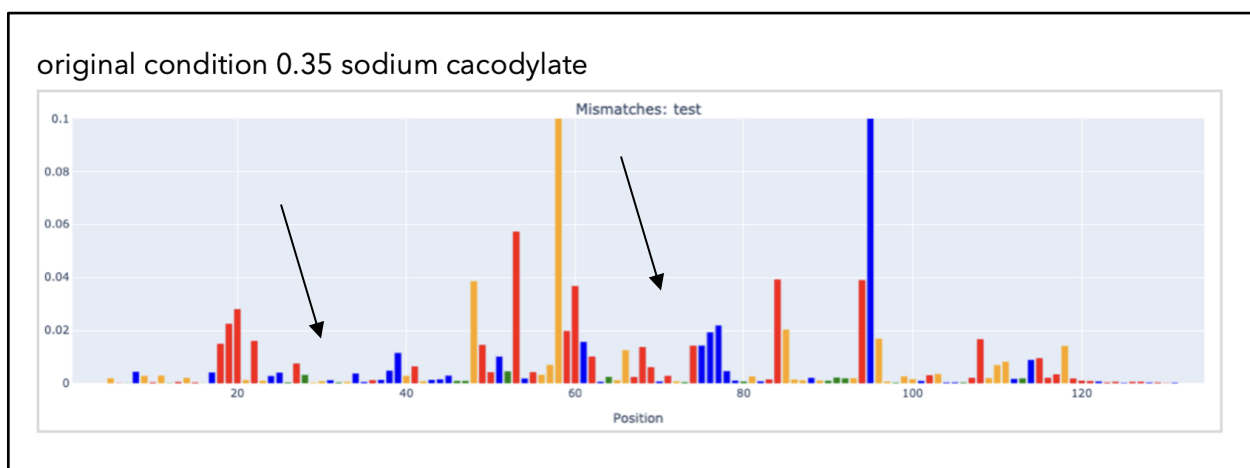
Figure 5A. Chemical mapping data using 0.35 M sodium cacodylate as a folding buffer. Modification of tertiary contacts are noted.
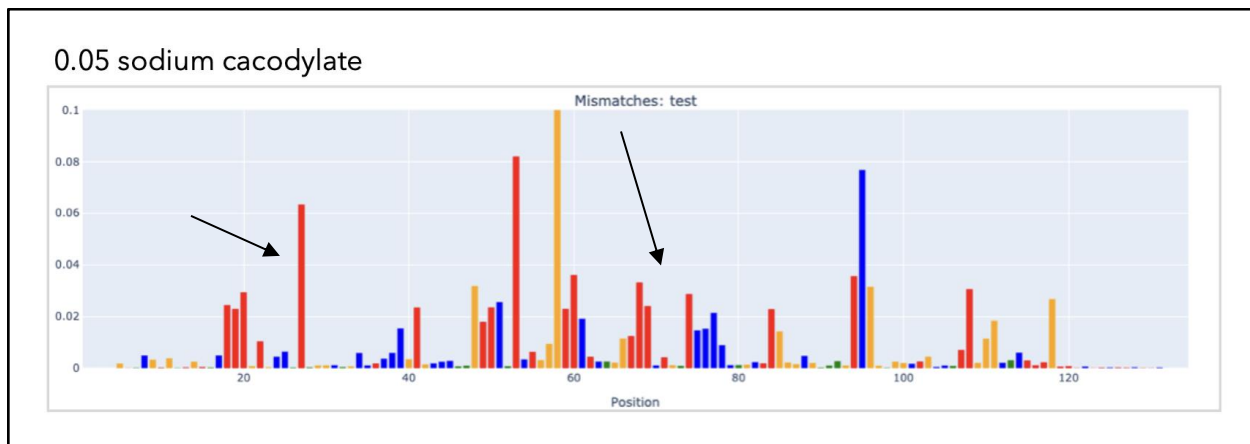

Figure 5B. Chemical mapping data using 0.05 M sodium cacodylate as a folding buffer. Modification of tertiary contacts are noted.

Figures 6A and 6B show chemical mapping results when HEPES is used as a folding buffer. HEPES is closer to biological conditions than sodium cacodylate, with a more neutral pH. Notable differences between results with HEPES and sodium cacodylate are represented in the modification of tertiary contacts. Negatively charged RNA ions resist methylation, but conditions with enough ions still allow for modification of tertiary contacts.
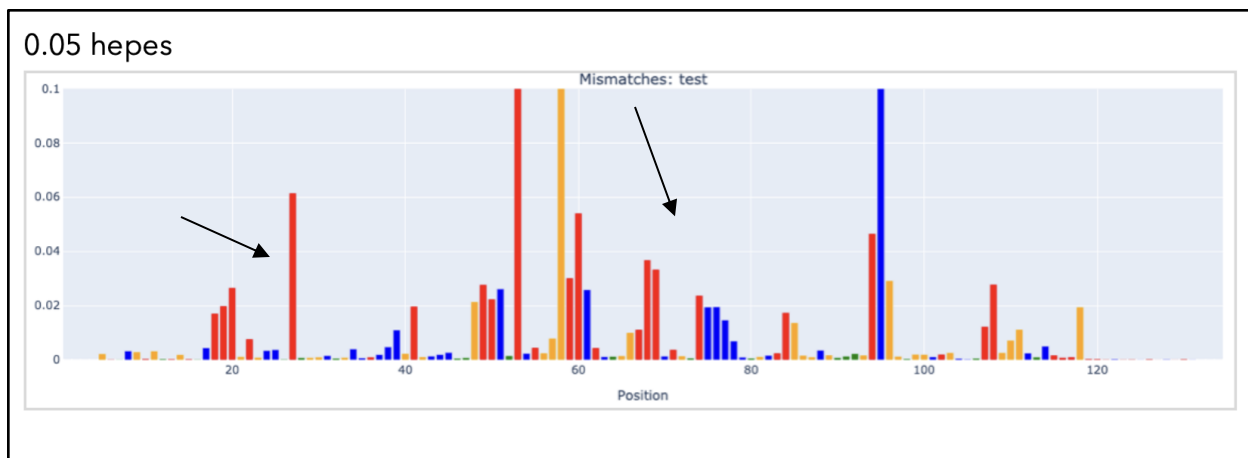

Figure 6A. Chemical mapping data using 0.05 M HEPES as a folding buffer. Modification of tertiary contacts are noted.
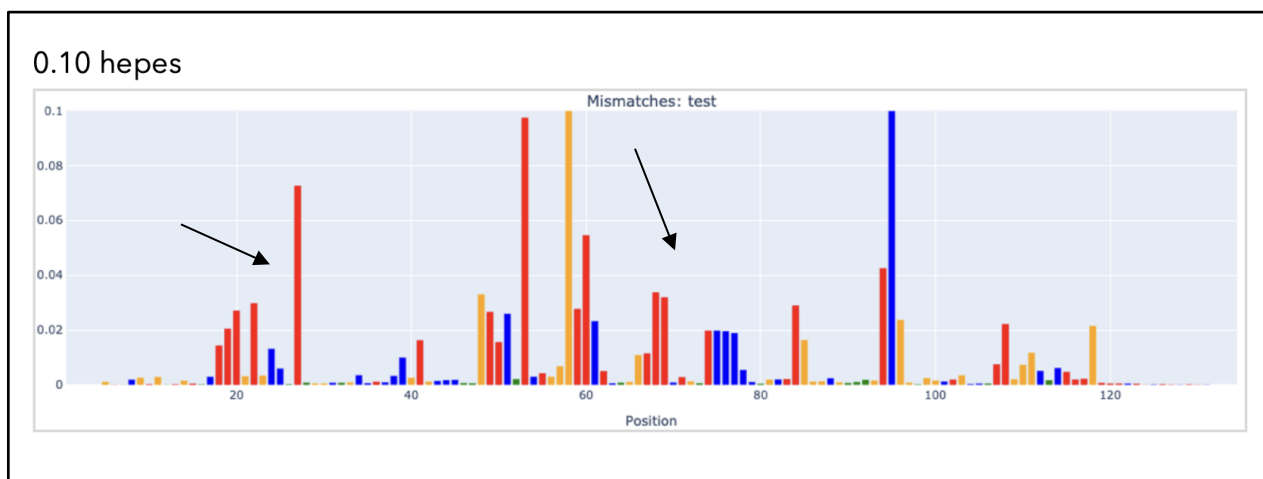

Figure 6B. Chemical mapping data using 0.10 M HEPES as a folding buffer. Modification of tertiary contacts are noted.

4. DNA processing via PCR and gel extraction.

Purification of DNA after PCR via gel extraction instead of PCR clean-up results in higher alignment between the target sequence and sequencing data. Sequence alignment of a particular construct is ~66% when DNA is purified after PCR using a PCR cleanup spin purification kit.

Sequence alignment of ~97% is seen in the same construct when DNA is purified using a gel extraction spin purification kit. The change from PCR cleanup kits to gel extraction purification kits allows for almost two times the amount of usable data to be analyzed. Standardizing gel extraction for all constructs shows a typical alignment rate between 95%-99% .

5. <u>Temperature during modification and folding.</u>

Although not detailed in the standardized experiment listed, much can be learned from folding and modifying RNA at different temperatures. Figure 7A shows an RNA construct at 35 C, while figure 7B shows the same construct at 45 C. These constructs were kept in these temperatures during modification and folding. Once modification was complete the constructs were worked with at room temperature. As temperature increases, modifications increase. It is important to note that this increases the background noise in the data in addition to the modifications expected to be seen from DMS. This should be considered when titrating higher temperatures for chemical mapping. As temperature increases, modification time should also decrease, with the highest temperatures between 50-60 degrees C having a modification time between 4-5 minutes instead of 6.
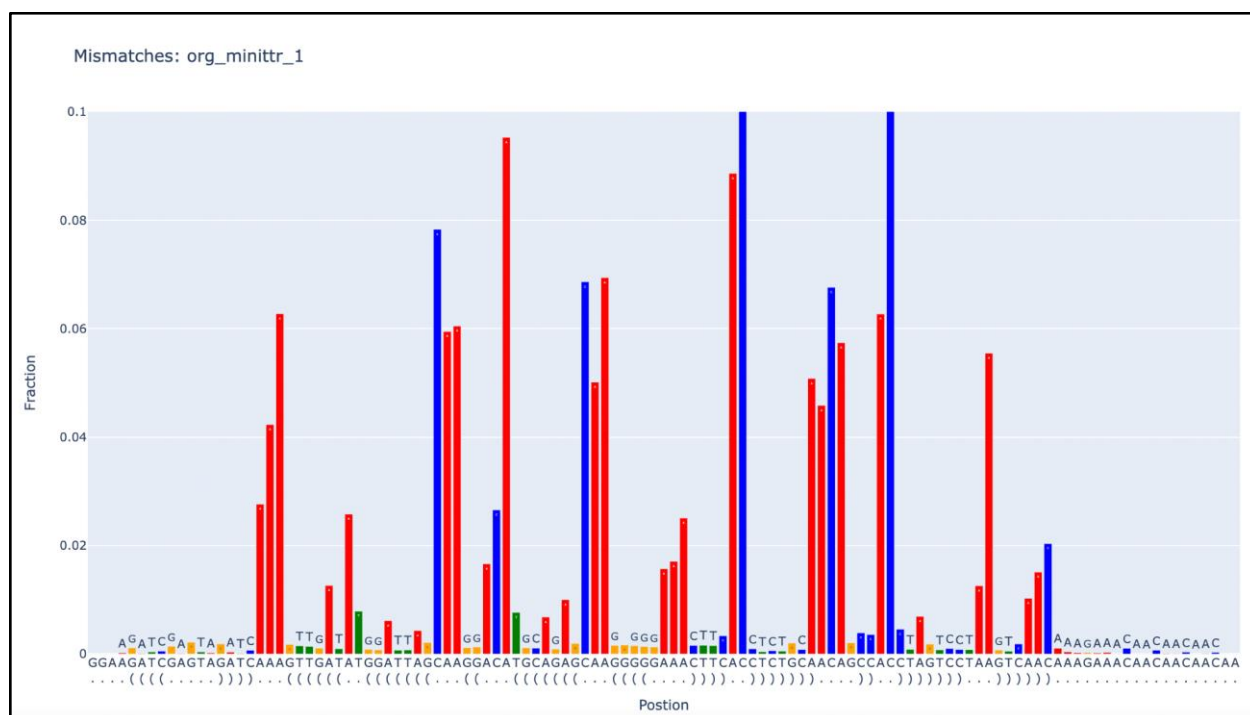

Figure 7A. Fraction of modifications for RNA construct at 35 degrees C.
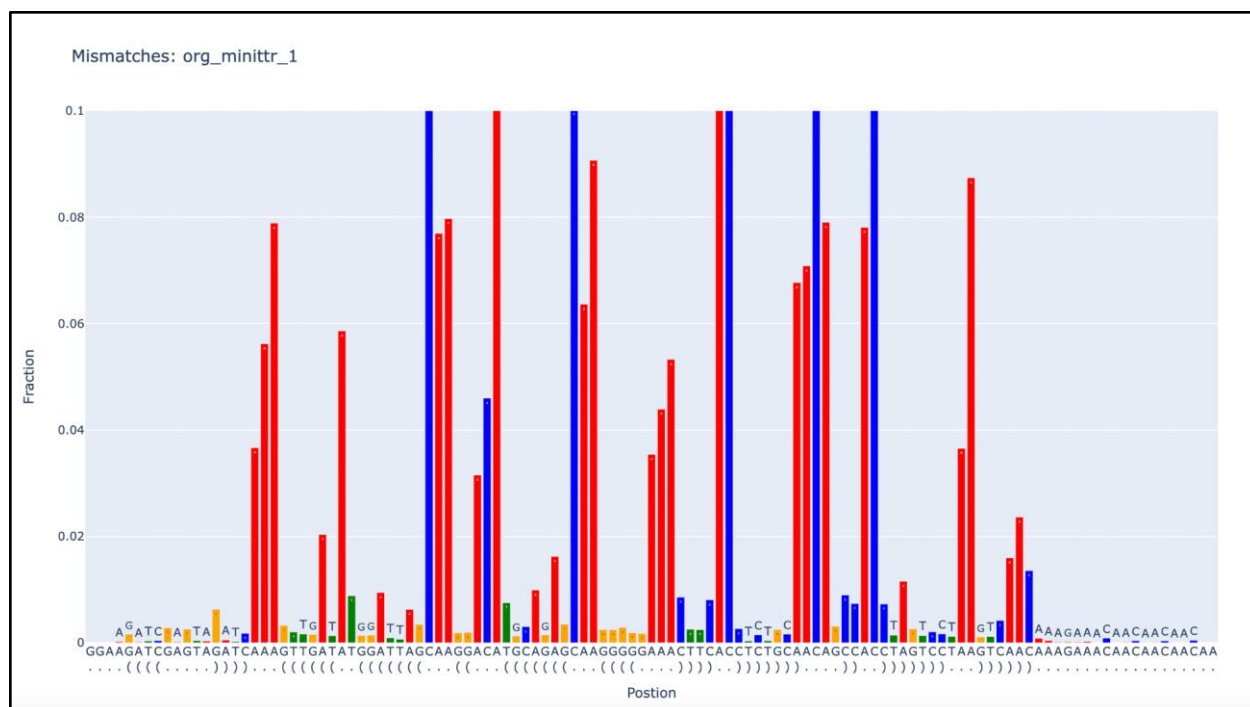
Figure 7B. Fraction of modifications for RNA construct at 45 degrees C. In comparison to Figure 7A, the percentage of modified bases is much higher.

Titrating variables & addition of ligands to determine optimal conditions for specific molecules
Protocols should be modified if variables such as temperature or modifier concentration are being tested. If temperature is to be titrated as a reaction variable, reaction time should decrease to observe cleaner data with less background noise after the sample is sequenced. The higher the temperature of the reaction, the faster it occurs. With higher temperatures or higher amounts of modifier, the modification time should decrease. Folding time should also take place at the temperature the construct will be modified at. If ligands are being added into the reaction, this should be done prior to modification and added with the folding buffer. 16.5 uL of folding buffer should be added with 1 uL of ligand. It is often valuable to complete data analysis on temperature titrations because the RNA folding is different at higher temperatures, and can often become less predictable. This would therefore impact the modifications of bases depending on exposure to reagent in solution.

Chemical mapping modifiers, such as 1M7 (1-methyl-7-nitroisatoic anhydride) modification via SHAPE protocols, can be used for chemical mapping purposes, although will lead to different

outcomes. 1M7 modifies all nucleotide bases, not just As and Cs. Ligands such as antibiotics and carbohydrates can be added to the reaction with a folding buffer to observe the impacts of these substances on folding and DMS reactivity.

Discussion

Alterations to original chemical mapping protocols for 3D RNA structure work include modification time, buffer conditions, increasing magnesium amounts used, and changes to purification methods. The results provide a recommendation for streamlining chemical mapping as a method of probing RNA tertiary structure. The formation of tertiary contacts can be observed based on the reactivity patterns from methylation via DMS. An ability to predict formation patterns off tertiary contacts allows an understanding of 3D RNA folding.

It is important to ensure all materials used, especially the DMS reagent and Qubit kits used for concentration measurements, are not degraded or expired. DMS side reactions can occur due to air exposure. It is recommended to keep a small DMS stock for chemical mapping purposes that is changed weekly to limit degradation. Oxidation of DMS due to air exposure decreases the reproducibility and accuracy of experimental results.

Structure is the biggest contributor to RNA function. Methods such as chemical mapping to elucidate 3D structure are relevant to the function of antibiotics and other pharmaceutical treatments at the molecular level. An understanding of the way antibiotics and other drugs interact with structural functional RNAs can lead to promising pharmaceutical applications. In bacteria, many structural RNAs are involved in cell-to-cell signaling. Functional impairment of these RNAs through drug use could provide a promising treatment option for bacterial infections. Future chemical mapping applications should continue to consider biological cell conditions. Potential treatments with a basis on in vivo RNA tertiary structure should be explored as a viable option for disease management and treatment.

Acknowledgements

I would like to acknowledge my primary investigator, Dr. Joe Yesselman, for his support, dedication, and time given to this experiment as well as advising writing for this thesis. I give my

References

1. Sharp, P. A. The Centrality of RNA. *Cell* **2009**, *136*, 577–580.

2. Leontis, N. B.; Lescoute, A.; Westhof, E. The Building Blocks and Motifs of RNA Architecture. *Curr. Opin. Struct. Biol.* **2006**, *16*, 279–287.

3. Kurreck, J. RNA Interference: From Basic Research to Therapeutic Applications. *Angew Chem Int Ed Engl* **2009**, *48*, 1378–1398.

4. Van Damme, R.; Li, K.; Zhang, M.; Bai, J.; Lee, W. H.; Yesselman, J. D.; Lu, Z.; Velema, W. A. Chemical Reversible Crosslinking Enables Measurement of RNA 3D Distances and Alternative Conformations in Cells. *Nat. Commun.* **2022**, *13*, 911.

5. Mustoe, A. M.; Lama, N. N.; Irving, P. S.; Olson, S. W.; Weeks, K. M. RNA Base-Pairing Complexity in Living Cells Visualized by Correlated Chemical Probing. *Proc Natl Acad Sci USA* **2019**, *116*, 24574–24582.

6. Homan, P. J.; Favorov, O. V.; Lavender, C. A.; Kursun, O.; Ge, X.; Busan, S.; Dokholyan, N. V.; Weeks, K. M. Single-Molecule Correlated Chemical Probing of RNA. *Proc Natl Acad Sci USA* **2014**, *111*, 13858–13863.

7. Das, R. RNA Structure: A Renaissance Begins? *Nat. Methods* **2021**, *18*, 439.